Role of Surface Lysine Residues of Adipocyte Fatty Acid-Binding Protein in Fatty Acid Transfer to Phospholipid Vesicles†

Heng-Ling Liou‡ and Judith Storch*

Department of Nutritional Sciences, Rutgers University, 96 Lipman Drive, New Brunswick, New Jersey 08901-8525

Received January 17, 2001; Revised Manuscript Received March 20, 2001

ABSTRACT: The tertiary structure of murine adipocyte fatty acid-binding protein (AFABP) is a flattened 10-stranded β-barrel capped by a helix−turn−helix segment. This helical domain is hypothesized to behave as a "lid" or portal for ligand entry into and exit from the binding cavity. Previously, we demonstrated that anthroyloxy-labeled fatty acid (AOFA) transfer from AFABP to phospholipid membranes occurs by a collisional process, in which ionic interactions between positively charged lysine residues on the protein surface and negatively charged phospholipid headgroups are involved. In the present study, the role of specific lysine residues located in the portal and other regions of AFABP was directly examined using site-directed mutagenesis. The results showed that isoleucine replacement for lysine in the portal region, including the αI- and αII-helices and the β C-D turn, resulted in much slower 2-(9-anthroyloxy)palmitate (2AP) transfer rates to acidic membranes than those of native AFABP. An additive effect was found for mutant K22,59I, displaying the slowest rates of FA transfer. Rates of 2AP transfer from "nonportal" mutants on the β-G and I strands were affected only moderately; however, a lysine → isoleucine mutation in the nonportal β-A strand decreased the 2AP transfer rate. These studies suggest that lysines in the helical cap domain are important for governing ionic interactions between AFABP and membranes. Furthermore, it appears that more than one distinct region, including the αI-helix, αII-helix, β C-D turn, and the β-A strand, is involved in these charge−charge interactions.

Adipocytes play a central role in lipid homeostasis and the maintenance of energy balance in vertebrates. During periods of excess energy intake, fatty acids are stored as triacylglycerol (TG)[1] in adipose tissue. During periods of energy deprivation, fatty acids (FA) are the major energy source for most tissues and are exported from the adipose tissue. The mechanisms by which FA are transported in the adipocyte are not precisely known; however, intracellular lipid-binding proteins are thought to play a role in fatty acid trafficking.

Adipocyte fatty acid-binding protein (AFABP), also known as adipocyte lipid-binding protein (ALBP) and aP2, is abundantly expressed in adipose tissue, comprising up to 6% of the total cytosolic protein in the cultured differentiated adipocyte (*1*). AFABP belongs to a family of small intracellular carriers (14−15 kDa) for hydrophobic ligands known as the fatty acid-binding proteins (FABP). The expression of AFABP is associated with adipocyte differentiation (*2*), and a role for AFABP in enhancing FA uptake has been suggested by studies in 3T3-L1 cultured adipocytes as well as studies in AFABP-transfected Chinese hamster ovary (CHO) cells (*3*−*5*). Recently, AFABP has also been suggested to be involved in the efflux of fatty acids out of adipocytes via its interaction with hormone-sensitive lipase (*6*).

To address the putative transport function of the FABPs, we have used an in vitro fluorescence resonance energy transfer assay to examine the rate and mechanism of anthroyloxy labeled fatty acid transfer from FABP to model membranes. The results suggested that several FABPs, including adipocyte FABP and heart FABP (HFABP), transfer fatty acids to acceptor phospholipid membranes via a collisional process, in which the protein is hypothesized to associate with membranes during ligand delivery (*7*−*9*). The rate-limiting step for FA transfer, therefore, appears to involve an effective physical interaction between the protein and the membranes, rather than the dissociation of FA into the aqueous phase, which appears to occur with LFABP (*9*) and CRBP type II (*10*).

A number of observations suggested that electrostatic interactions between AFABP and membranes may modulate the collisional FA transfer process. The headgroup charge of the acceptor membrane phospholipids markedly affects the rate of FA transfer (*11*). In addition, neutralization of the 14 lysine residues on the AFABP surface by chemical modification (acetylation) not only resulted in dramatically

† This work was supported by Grant DK38393 from the National Institute of Health (J.S.) and by Predoctoral Fellowship Award 9704048A (H.-L.L.) from the American Heart Association.

* To whom correspondence should be addressed: phone, 732-932-1689; fax, 732-932-6837; e-mail, storch@aesop.rutgers.edu.

‡ Present address: Center for Advanced Biotechnology and Medicine, Department of Pharmacology, UMDNJ-Robert Wood Johnson Medical School, 679 Hoes Lane, Piscataway, NJ 08854.

[1] Abbreviations: AFABP, adipocyte fatty acid-binding protein; HFABP, heart fatty acid-binding protein; FA, fatty acid; FABP, fatty acid-binding protein; AOFA, anthroyloxy-labeled fatty acid; 2AP, 2-(9-anthroyloxy)palmitic acid; EPC, egg phosphatidylcholine; PS, phosphatidylserine; CL, cardiolipin; NBDPC, 1-palmitoyl-2-[12-[(7-nitro-2,1,3-benzoxadiazol-4-yl)amino]dodecanoyl]-*sn*-glycero-3-phosphocholine; ADIFAB, acrylodated intestinal fatty acid-binding protein; WT-AFABP, wild-type adipocyte fatty acid-binding protein.

10.1021/bi0101042 CCC: $20.00
Published on Web 05/04/2001

decreased rates of fluorescent FA transfer but also altered the transfer mechanism from a collisional to a diffusional process (*12*). A series of recent studies using Fourier transform infrared (FTIR) spectroscopy, equilibrium binding, and a competitive binding assay have demonstrated direct interactions of AFABP with anionic phospholipid membranes and order-of-magnitude lesser interactions with zwitterionic membranes (*13*, *14*). Collectively, these studies indicate that electrostatic interactions are likely to be important in AFABP−membrane "collisions".

Despite disparate primary sequences (22−64% sequence identity) (*15*−*21*), members of the FABP family are characterized by remarkably similar tertiary structures, consisting of a 10-stranded antiparallel β-barrel capped by two short α-helices arranged as a helix−turn−helix motif (*17*, *22*−*24*). The α-helical domain covers one end of the binding cavity, and the αII-helix participates in a proposed "dynamic portal" that may regulate the entry and exit of fatty acids from the internal ligand binding cavity (*25*, *26*). Site-directed mutagenesis of lysines on the α-helical domain of HFABP, a homologous protein with greater than 60% sequence identity to AFABP, demonstrated that specific lysine residues on the α-helical segments, but not other regions, appeared to be involved in ionic interactions between HFABP and model phospholipid membranes (*27*). We nevertheless considered the possibility that the structural determinants of AFABP function might not be identical to those of HFABP because of certain different functional properties. In particular, AFABP transfers fluorescent FA to membranes at least 10-fold faster than HFABP (*11*). Further, AOFA transfer rates from A- and HFABP display different responses to aqueous phase ionic strength (*28*). X-ray crystallographic structures also show that the FA conformations in the binding sites of the two proteins are different (*29*, *30*). Thus, despite the fact that A- and HFABP have high sequence identity and several consensus lysine residues, the large differences in absolute AOFA transfer rates as well as their differential regulation by aqueous phase properties prompted us to investigate the effect of conserved and unique lysine residues in AFABP on the process of FA transfer to membranes to further define the structure−function relationships for AFABP and the FABP family of proteins.

The objective of this study was to determine the specific lysine residues and regions of AFABP which are involved in putative electrostatic interactions between the protein and phospholipid membranes during fatty acid transfer. The results demonstrate that the portal domain, which includes the helix−turn−helix motif as well as the turn between β-strands β-C and β-D, is an important determinant of the absolute rate of FA transfer from AFABP to membranes. Additionally, the β-A strand in the nonportal region also plays a role in the process of ligand transfer.

EXPERIMENTAL PROCEDURES

Materials. The expression vector for wild-type murine AFABP (pET-AFABP) was generously provided by Dr. Alan Kleinfeld (Medical Biology Institute, La Jolla, CA). Competent BL21 (DE3) cells and vector pET-11a for mutant protein expression were from Novagen (Milwaukee, WI). Restriction enzymes *Xba*I and *Bam*HI and deoxynucleotides (dNTP) were purchased from Promega (Madison, WI). Vent polymerase for PCR was purchased from New England Biolabs, Inc. (Beverly, MA). The in vitro mutagenesis kit and T4 polynucleotide kinase were from Amersham, Inc. Oligonucleotides and primers containing mutations were purchased from Midland Certified Reagents (Midland, TX). The QIAprep-spin plasmid kit and QIAEXII DNA gel extraction kit were obtained from Qiagen, Inc. (Valencia, CA). Tryptone, yeast extract, ampicillin, kanamycin, and quinine sulfate were purchased from Sigma Chemical Co. (St. Louis, MO). The fluorescent fatty acid analogue 2-(9-anthroyloxy)palmitate (2AP) and ADIFAB (acrylodated intestinal FABP) were from Molecular Probes, Inc. (Eugene, OR). Oleate (sodium salt) used for the ADIFAB assay was purchased from Nu-Chek Prep (Elysian, MN). Egg phosphatidylcholine (EPC), 1-palmitoyl-2-[12-[(7-nitro-2,1,3-benzoxadiazol-4-yl)amino]dodecanoyl]-*sn*-glycero-3-phosphocholine (NBD-PC), brain phosphatidylserine (PS), and bovine heart cardiolipin (CL) were obtained from Avanti Polar Lipids (Alabaster, AL).

Table 1: Oligonucleotide Primers for Mutagenesis[a]

mutation Lys → Ile	primers	underlined	sequences 5′ → 3′
outermost	HL06	*Bam*HI	GGCGGCCGCTCTAGAAATAATT
	HL09	*Xba*I	CCGGGGGATCCTAATTTCCATC
K59I	HL04	antisense	CTCGGTGTTTATAAAAGTACT
K22I	HL07	antisense	CACTCCCACTTCTATCATGTAATC
	HL08	sense	GATTACATGATAGAAGTGGGAGTG
K32I	HL05	antisense	GCCTGCCACTATCCTTGTGGC
	HL10	sense	GCCACAAGGATAGTGGCAGGC
K10I	HL11	antisense	GGAGACAAGTATCCAGGTTCC
	HL12	sense	GGAACCTGGATACTTGTCTCC
K97I	HL13	antisense	TCCATCCCATATCTGCACCTG
	HL14	sense	CAGGTGCAGATATGGGATGGA
K113I	HL15	antisense	TTCCACCAGTATGTCACCATC
	HL16	sense	GATGGTGACATACTGGTGGAA

[a] Oligonucleotide primers bearing lysine (AAA) to isoleucine (ATA) mutations were from Midland Certified Reagents (Midland, TX). All primers are listed from the 5′ to 3′ end. Primer HL04 was needed for K59I mutagenesis generated by in vitro mutagenesis protocol. Two outermost primers HL06 and HL09 were utilized to synthesize the full-length DNA fragment. The underlined sequences in oligos HL06 and HL09 represent *Xba*I and *Bam*HI sites, respectively, used for further subcloning.

Construction of Mutant AFABP Genes. A series of lysine to isoleucine (K → I) point mutants were constructed. Isoleucine was chosen to replace lysine due to its neutral charge and the relatively similar bulkiness to lysine, so as to maintain the backbone size of the protein. Seven mutations in six distinct regions of AFABP were investigated for their effects on FA transfer from AFABP to zwitterionic and anionic phospholipid model membranes. Four of the mutations were introduced in the portal region (helix−turn−helix and β-2 turn), and three of the substituted isoleucines were on different β-strands, β-A, β-G, and β-I, which are not in the putative portal region (Table 1). The numbering of amino acid residues was counted with the first methionine included. All mutants were constructed by overlapping polymerase chain reaction (PCR) (*31*) except mutant K59I which was initially constructed by the phosphothioate-based in vitro mutagenesis protocol (Amersham, Inc.). Oligo primers bearing mismatches to wild-type cDNA, indicated by underline, are listed in Table 1, from lysine (AAA) to isoleucine (ATA). Each mutation was verified by sequence analysis (*32*). Mutant DNA was subcloned into the pET-

11a expression vector by using the *Xba*I and *Bam*HI restriction sites.

Protein Purification. Wild-type and mutant AFABPs were purified from an *Escherichia coli* expression system as previously described (*14*). Briefly, pET constructs were transformed into the *E. coli* host strain BL21 (DE3), and protein expression was induced by the addition of 0.5 mM IPTG to the growing culture. The cells were harvested and resuspended in lysis buffer, and the cytosolic FABP was released by sonication. The resulting sample was centrifuged for 30 min at 40000*g*. The supernatant was applied to two sequential size-exclusion Sephadex G-50 columns: anion-exchange chromatography (DE 52 column, Whatman) and delipidation (Lipidex 1000, Sigma). FABP purity was assessed by SDS−PAGE. Protein concentration was calculated using the molar extinction coefficient for AFABP at 280 nm, 1.36×10^4 M^{-1} cm^{-1} (*33*).

Control Analysis of FABP Structural Integrity. The following methods were utilized to examine the integrity of mutant AFABP structure and physical properties to ensure that the point mutations introduced did not change the overall protein conformation and/or its ligand-binding properties.

(A) Circular Dichroism. Circular dichroism (CD) spectra were measured to verify that no overall folding modifications occurred in the mutant FABP structures as previously described (*27*). Secondary structure analysis was performed with a least-squares fitting program utilizing the protein secondary structural analysis of Yang et al. (*34*) and Chang et al. (*35*).

(B) Geometry Minimization. Energy minimization was used to compare the mutant AFABP structures with the wild-type protein to ensure that no large structural differences in the local region surrounding the mutation, as well as for the entire protein, would occur. For the local minimization, seven residues (the mutated residue ± three) and bound water molecules were selected, and the lowest free energy for this domain was determined using Hyperchem software (Hypercube, Inc., Gainesville, FL). For the entire protein, the free energy including water molecules was determined using software Discover and Insight II provided by Silicon Graphics Inc. (MSI, San Diego, CA).

(C) Fluorescence Measurements. To check the hydrophobicity of the internal ligand-binding pocket, fluorescent quantum yields (Q_f) of the fluorescent fatty acid analogue 2AP bound to wild-type or mutant AFABP were determined with an SLM 8000C fluorescence spectrophotometer as previously described (*36*). Excitation wavelengths were set at 383 nm for 2AP and 352 nm for quinine sulfate in 0.1 N H_2SO_4 (reference fluorophore, $Q_{ref} = 0.7$).

(D) Binding of FA to AFABPs. Binding of oleate to wild-type and mutant AFABPs was analyzed by employing the fluorescent probe ADIFAB (*33*, *37*), as previously described, to obtain the values of K_d for oleate binding, as well as the binding stoichiometry (*27*).

Vesicle Preparation. Small unilamellar vesicles (SUVs) were prepared by sonication and ultracentrifugation as previously described (*38*) in TBS buffer (40 mM Tris-HCl, 100 mM NaCl, pH 7.4) except for SUVs containing cardiolipin which were prepared in TBS with 1 mM EDTA. The standard vesicles were prepared to contain 90 mol % of EPC and 10 mol % of NBDPC, which served as the zwitterionic fluorescence quencher. To introduce the negative charge into model vesicles, either 25 mol % of phosphatidylserine (PS) or cardiolipin (CL) was incorporated into the neutral SUVs in place of an equimolar amount of EPC. The phospholipid concentrations were determined by quantitation of inorganic phosphate (*39*), and CL-containing vesicles have been corrected for two phosphate groups per CL molecule.

Transfer of 2AP from AFABP to Model Membranes. The rate of 2AP transfer from wild-type and mutant AFABPs to acceptor vesicles was determined using a fluorescence resonance energy transfer assay as detailed previously (*14*). FA transfer was monitored at 25 °C in TBS buffer. The conditions were developed prior to each experiment to ensure that no photobleaching of AOFA was observed. Final concentrations in a typical transfer assay were 10 μM AFABP, 1 μM 2AP, and 100−500 μM vesicles. The fluorescent FA−FABP complex was the fluorescence donor. Upon mixing of the FA−FABP complex with acceptor membranes, transfer of FA from protein to acceptor SUVs is directly monitored by the time-dependent decrease in fluorescence, using an SX-18MV stopped-flow spectrofluorometer (Applied Photophysics Ltd., U.K.) interfaced with an Acorn A5000 computer. The data were analyzed as previously described by fitting to a single exponential with steady-state function (*14*).

Statistical Analysis. In each transfer experiment, seven replicates of each condition were collected. Results are presented as mean ± standard error of the mean (SEM) for three or more separate sets of experiments. Two tail paired *t*-test was used to analyze the differences between rates of FA transfer from mutant proteins versus wild-type AFABP to various concentrations and compositions of phospholipid membranes. Results were considered statistically significant at $p < 0.05$.

RESULTS

Controls for Conformational Integrity of Mutant Proteins. Circular dichroic spectra showed no major differences in mutant proteins relative to wild-type AFABP, indicating no substantial alteration introduced by mutation in the overall folding of the β-barrel structure. The CD spectra obtained from wild-type and mutant proteins were almost superimposable, demonstrating curves typical of proteins with a large content of β-sheet. The molar ellipticity at 222 nm, θ_{222}, for wild-type protein was approximately −8127 deg cm^2/dmol and ranged from −7446 to −9144 deg cm^2/dmol for various mutants, indicating a similar α-helical content (Table 2). All proteins contained 68−71% β-sheet in overall secondary structure, when spectra were analyzed using the reference spectra of Chang et al. (*35*), indicating the maintenance of the β-barrel structure in the mutant proteins. This analysis of secondary structure is also consistent with the X-ray crystal structure of AFABP (*17*, *18*), which shows 70% and 20% of protein content in the β-sheet and α-helical conformation, respectively.

Free energy minimization estimations of mutant AFABPs were determined both for the local region adjacent to the mutation site and for the entire mutant protein, compared with the wild-type protein. As shown in Table 3, for the 7-residue domain and sphere water molecules surrounding each mutation, the increases in ΔG were less than 0.37%, except for K22I which increased by 1.47%. Likewise, the

Table 2: Physical and Binding Properties of Wild-Type and Mutant AFABPs[a]

protein	θ_{222} (deg cm^2/dmol)	β-sheets (%)	K_d (nM)	binding site (n)	quantum yield (Q_f)
A-WT	−8127	71	110 ± 11	1.2 ± 0.1	0.27 ± 0.01
K22I	−8154	70	146 ± 11	1.2 ± 0.1	0.26 ± 0.03
K32I	−7451	71	119 ± 8	1.1 ± 0.1	0.26 ± 0.02
K59I	−8034	69	69 ± 8	1.3 ± 0.1	0.26 ± 0.01
K22,59I	−7821	71	68 ± 7	0.9 ± 0.1	0.23 ± 0.01
K10I	−9144	70	109 ± 3	1.1 ± 0.1	0.26 ± 0.03
K97I	−7446	68	85 ± 8	1.1 ± 0.1	0.28 ± 0.03
K113I	−8538	70	89 ± 10	1.2 ± 0.1	0.27 ± 0.03

[a] Circular dichroism spectroscopic properties were determined as described in Experimental Procedures. The ellipticity for α-helical content, θ_{222}, was determined as per Chang et al. (*35*). Measurement of fluorescence quantum yield for 2AP was repeated at least three separate times, and results are shown as mean ± SEM for fatty acid-binding analysis. Recombinant AFABP was titrated with oleate, and ligand binding was assessed using the ADIFAB assay (n = 5). Final concentrations were 4 μM AFABP, 0.2 μM ADIFAB, and 0−5 μM oleate, as described under Experimental Procedures. Results are presented as mean ± SEM.

Table 3: Local Energy Minimization of Wild-Type and Mutant AFABPs[a]

position	energy (kcal/mol) wild type (Lys)	mutant (Ile)
10 (β-A strand)	540.19	541.94
22 (αI-helix)	518.06	525.56
32 (αII-helix)	526.49	528.42
59 (β C-D turn)	533.66	534.70

[a] Energy minimization was calculated for a selected local region adjacent to the mutated residue. The mutated residue is in the middle of a total of seven selected amino acids. Lysine and isoleucine 10, 22, 32, and 59 on β-A strand, αI-helix, αII-helix, and β C-D turn were examined, respectively, using the Hyperchem program (Hypercube, Inc., Gainesville, FL).

Table 4: Free Energy Estimations of Wild-Type and Mutant AFABPs[a]

protein	energy (kcal/mol)
A-WT	608.81
A-K22I (αI-helix)	613.65
A-K32I (αII-helix)	607.43
A-K59I (β C-D turn)	616.94
A-K22,59I (αI-helix and β C-D turn)	620.95
A-K10I (β-A strand)	609.75
A-K97I (β-G strand)	615.19
A-K113I (β-I strand)	614.00

[a] Free energy minimization was calculated for an entire protein, for native and mutant AFABPs, using the programs Insight II and Discover from Silicon Graphics Inc. (MSI, San Diego, CA).

differences in overall free energy of each mutant protein compared with native AFABP were also small, ranging from 0.15% to 1.99% (Table 4). Thus, these estimations of energy minimization suggest that, as anticipated, the point mutations did not change the protein structure to a great extent.

The integrity of the ligand-binding environment with K → I mutation was expected to be maintained, as the tertiary structure indicates that the side chains of lysine residues of AFABP face the aqueous environment rather than pointing into the interior of the ligand-binding cavity (*18*). AOFA probe 2AP quantum yield (Q_f) was measured to examine the hydrophobic environment of the FA binding pocket in wild-type and mutant proteins (*36*). The value of Q_f for native AFABP was 0.27 ± 0.01 (Table 2). The values for the AFABP mutants ranged from 0.23 to 0.28, confirming that the mutagenesis of surface lysine residues did not change the hydrophobicity of the interior ligand binding cavity of AFABP.

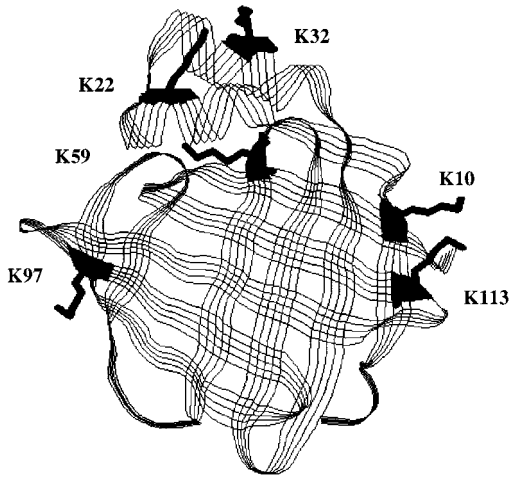

FIGURE 1: Ribbon diagram of adipocyte fatty acid-binding protein. Representation of the X-ray crystal structure of AFABP determined by Xu et al. (*18*). The selective lysine K → I point mutations in the present study are highlighted as black sticks on the protein backbone.

The dissociation constant (K_d) for binding of oleate to wild-type and mutant AFABPs was assessed using the fluorescent probe ADIFAB, as previously described (*27*). The dissociation constant for oleate binding to wild-type AFABP was consistently found to be 110 ± 11 nM, which is somewhat higher than the 47 and 67 nM values reported earlier by Richieri et al. (*33*, *40*). The absolute K_d values obtained for mutants ranged from 68 ± 7 to 146 ± 11 nM (Table 2), indicating relatively small differences in FA-binding affinity relative to wild-type AFABP. The binding stoichiometry of native and mutant AFABPs to FA appeared to be 1 (Table 2), in agreement with the X-ray crystal structure (*18*) and earlier ADIFAB studies (*33*).

Effect of K → I Mutations on FA Transfer to Zwitterionic Phospholipid Membranes. The absolute rates of FA transfer from wild-type and mutant proteins to increasing concentrations of neutral EPC vesicles are shown in Figure 2. The transfer rate of 2AP from 10 μM wild-type AFABP (WT-AFABP) to 100 μM zwitterionic EPC vesicles was 1.83 ± 0.03 s^{-1}, and transfer to 500 μM SUV was approximately 4-fold faster, 6.5 ± 0.7 s^{-1}. Mutation K32I on the αII-helix resulted in 2−3-fold faster rates (p < 0.05) of FA transfer, ranging from 4.7 ± 0.6 to 21.8 ± 2.3 s^{-1} for 100 and 500 μM SUV, respectively. In contrast, other point mutations located in the portal region (K22I, K59I, and K22,59I) showed only minimal, if any, differences (10−20%) in absolute FA transfer rates. A small (30%) but statistically significant increase in rate (p < 0.05) was observed from "nonportal" mutant K10I to 500 μM neutral vesicles, while "nonportal" mutants K97I and K113I did not show any significant effects. The absolute rate of 2AP transfer (1.83 s^{-1}) was lower than our previous estimates of transfer rates to EPC/NBDPE acceptor vesicles (7.3 ± 0.5 s^{-1}) (*12*), under the same final conditions of protein:probe:SUV (10 μM:1 μM:100 μM), owing to the present incorporation of 10 mol % of the neutral quencher NBDPC into acceptor vesicles

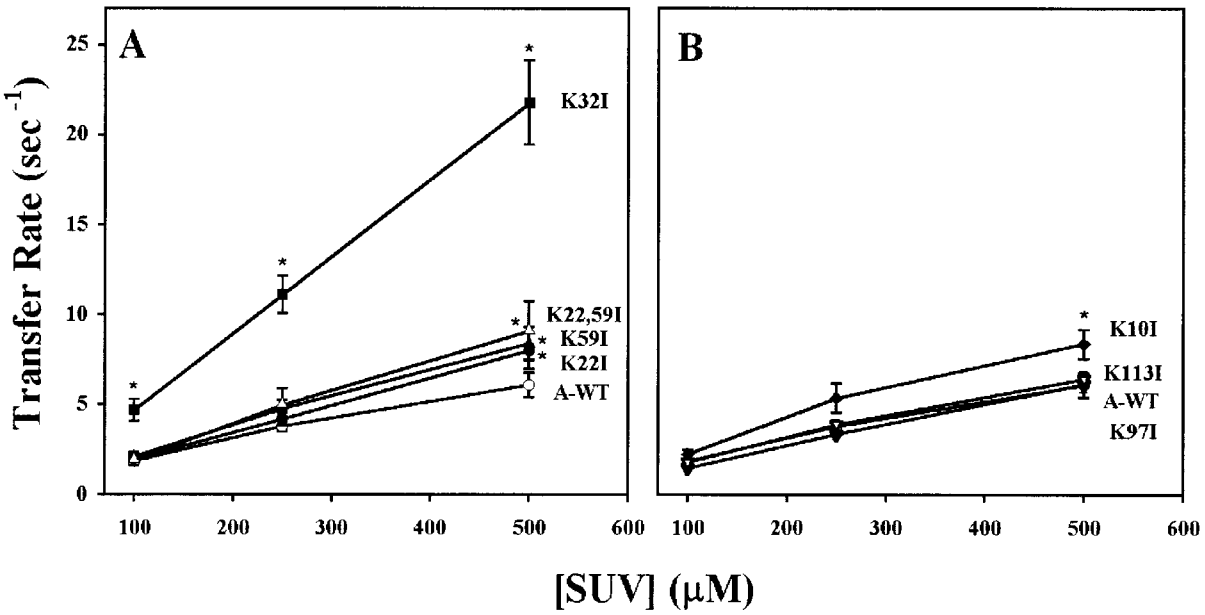

FIGURE 2: 2AP transfer from AFABP to zwitterionic membranes. The transfer of 2AP from wild-type AFABP and various mutants to SUV was measured at 25 °C, pH 7.4, as described in Experimental Procedures. Final concentrations were 10 μM AFABP with 1 μM probe and 100−500 μM EPC/NBDPC (90%/10% mol/mol) acceptor vesicles. (A) 2AP transfer from wild-type AFABP (○) and portal mutants K22I-AFABP (●), K32I-AFABP (■), K59I-AFABP (▲), and K22,59I-AFABP (△). (B) FA transfer from wild type (○) and nonportal mutants K10I-AFABP (◆), K97I-AFABP (▼), and K113I-AFABP (▽). The values of mean ± SEM were obtained from at least three separate sets of experiments. Two tail paired *t*-tests were used to determine the significant differences for each mutant vs wild-type AFABP. p value < 0.05 is presented as (*).

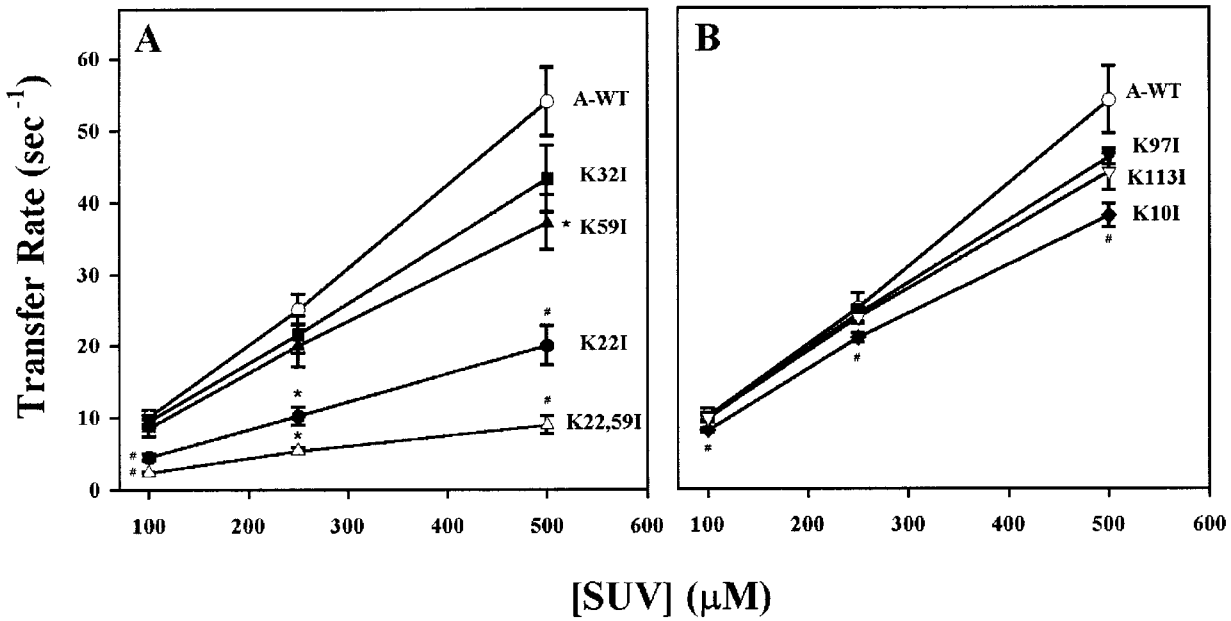

FIGURE 3: 2AP transfer from AFABP to phosphatidylserine-incorporated membranes. The transfer of 2AP from wild-type AFABP and various mutants to SUV was measured at 25 °C, pH 7.4, as described in Experimental Procedures. Final concentrations were 10 μM AFABP with 1 μM probe and 100−500 μM EPC/PS/NBDPC (65%/25%/10% mol/mol/mol) acceptor vesicles. (A) 2AP transfer from wild-type AFABP (○) and portal mutants K22I-AFABP (●), K32I-AFABP (■), K59I-AFABP (▲), and K22,59I-AFABP (△). (B) FA transfer from wild type (○) and nonportal mutants K10I-AFABP (◆), K97I-AFABP (▼), and K113I-AFABP (▽). The values shown are the mean ± SEM from three sets of experiments. p value < 0.05 (*) and p value < 0.01 (#) are presented.

instead of the negatively charged NBDPE used in the earlier studies (*12*, *27*).

Effect of K → I Mutations on Transfer to Anionic Membranes. As previously found (*11*), the absolute rates of 2AP transfer from native AFABP to membranes increased with the incorporation of negatively charged phospholipids (Figures 3 and 4). A 5-fold increase for WT-AFABP, on average, was observed in the absolute rates of 2AP transfer to increasing concentrations of PS-containing vesicles, ranging from 10.1 ± 1.0 to 54.1 ± 4.8 s^{-1} for transfer to 100 and 500 μM acceptor SUV, respectively (Figure 3). Like the native AFABP, all of the mutant forms also displayed an increase in the rate of 2AP transfer to PS vesicles; however, the observed absolute transfer rate constants were smaller for the mutants than for the wild-type protein. For example, changing lysine 22 on the αI-helix in mutant K22I-AFABP led to a 2−3-fold decrease in absolute rates of fatty acid transfer compared to the WT-AFABP. Neutralization

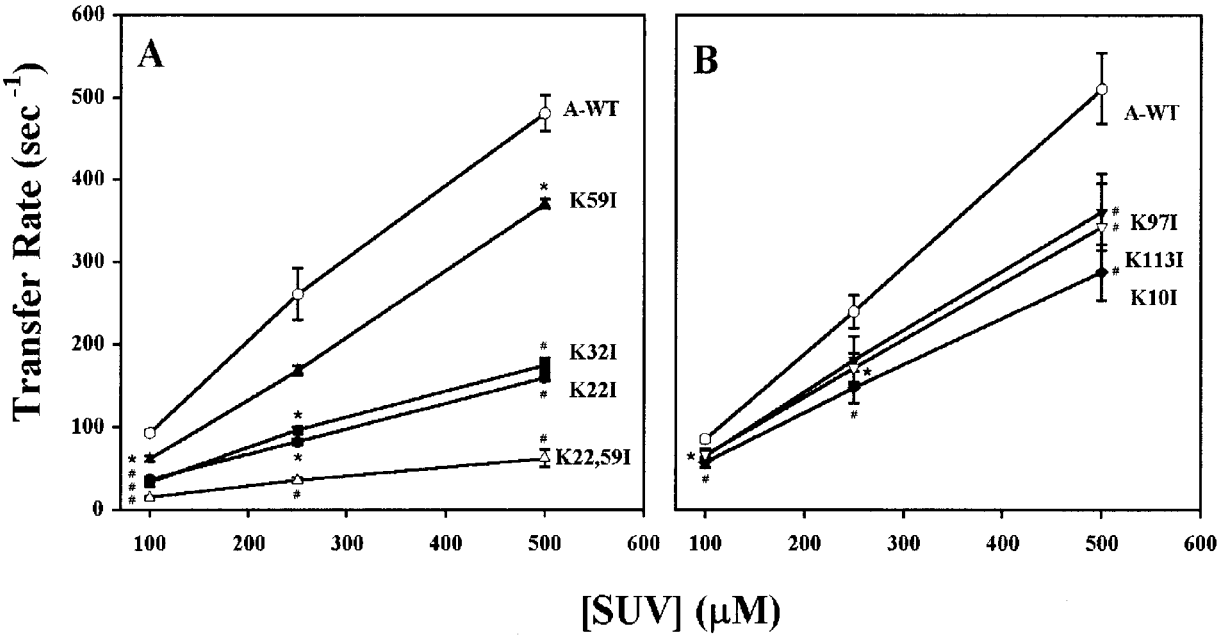

FIGURE 4: 2AP transfer from AFABP to cardiolipin-incorporated membranes. The transfer of 2AP from wild-type AFABP and various mutants to SUV was measured as previously described in Experimental Procedures. Final concentrations were 10 μM AFABP with 1 μM probe and 100−500 μM EPC/CL/NBDPC (65%/25%/10% mol/mol/mol) acceptor vesicles. (A) 2AP transfer from wild-type AFABP (○) and portal mutants K22I-AFABP (●), K32I-AFABP (■), K59I-AFABP (▲), and K22,59I-AFABP (△). (B) FA transfer from wild type (○) and nonportal mutants K10I-AFABP (◆), K97I-AFABP (▼), and K113I-AFABP (▽). The values of average ± SEM were obtained from three sets of experiments. p value < 0.05 (*) and p value < 0.01 (#) are presented.

of lysine 59 on the β C-D turn (mutant K59I-AFABP) displayed a small decrease of approximately 30% in FA transfer rates to PS-containing SUV, with the only significantly lower rates found at 500 μM SUV ($p < 0.05$). The K32I mutant showed small decreases (10−20%) relative to rates from WT-AFABP; however, the differences did not reach statistical significance.

FA transfer rates from a double mutant K22,59I-AFABP, containing mutations on both the αI-helix and β C-D turn, were 4−6-fold lower than those from WT-AFABP (Figure 3A), the slowest observed among all mutants. The effects of the K22,59I double mutation were essentially an additive function of the effects of each of the single mutations, suggesting that both the αI-helix and the β-turn between the C and D strands are determinants of the absolute rates of ligand transfer from AFABP. Although the transfer rates from mutant K22,59I were very slow, the observed mechanism of FA transfer from this protein remained a collisional process, in that the rates of transfer increased in direct proportion to the concentration of acceptor vesicles. Figure 3B shows the results of neutralization of the positive charge of lysines located in several nonportal regions, specifically β-strands A, G, and I. Isoleucine replacement in residue 10 (β-A) resulted in significantly lower transfer rates (≈30%) ($p < 0.01$), whereas the other two mutations in residues 97 (β-G) and 113 (β-I) decreased the rates by ≈20%; however, these differences did not reach statistical significance.

Incorporation of negatively charged CL in acceptor phospholipid vesicles resulted in a dramatic increase in AOFA transfer rate from AFABP relative to transfer from zwitterionic vesicles, consistent with earlier findings (*12*). In the present study, 2AP transfer rates from WT-AFABP to CL-containing vesicles were approximately 50-fold and 10-fold faster than those to zwitterionic and PS vesicles, respectively (Figure 4). In contrast with native AFABP, K → I mutant proteins demonstrated reduced levels of enhancement of ligand transfer to CL-containing vesicles, displaying similar transfer patterns as with the PS vesicles. For example, neutralization of single residues K59 and K22, and of these two sites together, resulted in approximately 30%, 3-fold, and 6−8-fold decreases in 2AP transfer rates relative to the wild-type AFABP ($p < 0.05$ or lower), respectively (Figure 4A). The additive effects of the K59 and K22 mutations once again point to the contribution of both the β C-D turn and the αI-helix to the collisional FA transfer process. Similar to results with the PS vesicles, small (20−40%) but statistically significant reductions ($p < 0.05$ or 0.01) in rates of 2AP transfer from the mutant proteins K97I-, K113I-, and K10I-AFABP to CL vesicles were found, relative to WT-AFABP (Figure 4B). The diminution of absolute rate of FA transfer was generally less from nonportal mutants than that from portal mutants. In contrast to the small effect (10−20%) of the K32I mutation on FA transfer to PS-containing membranes, transfer to CL-containing membranes was 3-fold slower than transfer from the wild-type AFABP. This suggests that, for CL in particular, the αII-helix is also involved in the process of FA transfer to phospholipid vesicles and that K32 may interact in possibly a unique way in comparison with other lysine residues investigated.

Sensitivity of Lysine Mutants to Phospholipid Negative Charge. To explore the sensitivity of each mutant to vesicle charge, the data are presented as the fold increase in 2AP transfer rate to PS or CL vesicles versus the transfer rate to neutral SUVs. For example, as shown in Figures 2−4, the transfer rate of 2AP from native AFABP to PS- and CL-containing vesicles increased 5- and 50-fold, respectively, when compared to transfer to neutral vesicles. The fold increase for each mutant was then compared to the increase observed for wild-type AFABP, by setting WT-AFABP to be 100% sensitivity. The results shown in Figure 5 are for

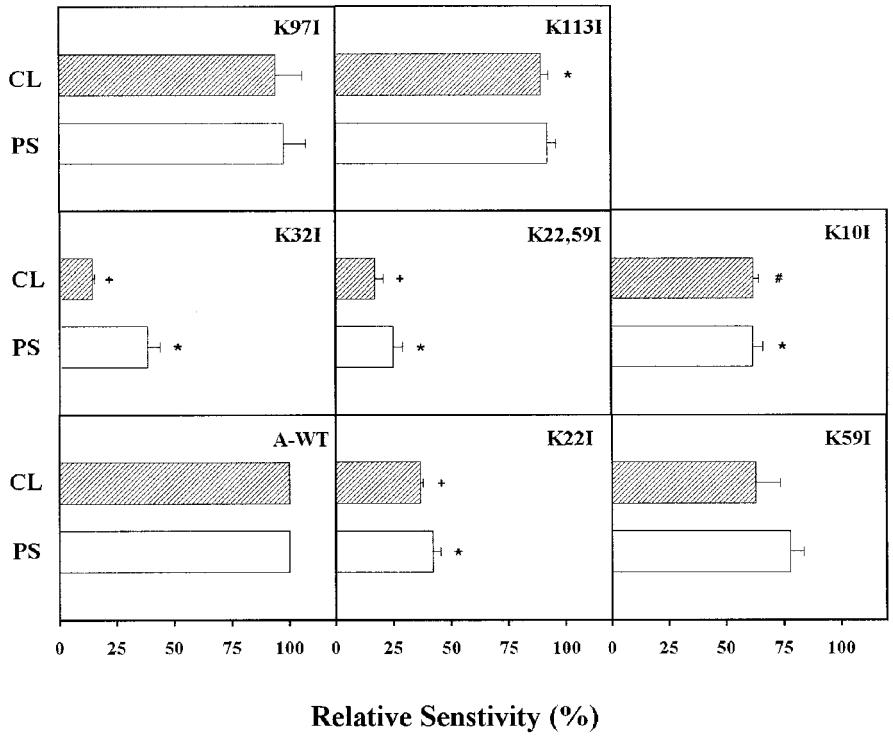

FIGURE 5: Effect of mutation on response to vesicle negative charge. The sensitivity of each K → I mutant protein to anionic vesicles is shown in the histogram. Key: PS vesicles (open bar) and CL vesicles (hatched bar). The graph is presented to show the relative sensitivity of mutants compared to that of wild-type AFABP (in percentage; i.e., the response of WT-AFABP to SUV is 100%). The values of the mean ± SEM are from three separate sets of experiments. Two tail paired *t*-test was used to determine the significant difference of each mutant vs wild-type AFABP. p value < 0.05 is shown as (*), $p < 0.01$ is shown as (#), and $p < 0.005$ is shown as (+).

100 μM SUV as a representative acceptor membrane concentration, and the effects were essentially identical for other vesicle concentrations.

Abolishment of positive charges in the helical domain of AFABP resulted in a substantial effect on the ability of the protein to sense the negative charges of the acceptor vesicles. Neutralization of the lysine residues in the αI- (K22I) and αII- (K32I) helices was found to reduce by at least 60−80% the increases of 2AP transfer rate to negatively charged relative to zwitterionic membranes (Figure 5). Modification of lysine 59, in the β C-D turn, resulted in a 25−40% reduction in sensitivity, and the double mutant K22,59I once again displayed a cumulative effect, with a decrease in sensitivity to negatively charged membranes of approximately 75−85% relative to the sensitivity of the WT-AFABP. The sensitivity to negative charge of nonportal mutants K97I and K113I was less than that of the helical domain mutants. K97I-AFABP (β-G strand) appeared to resemble the WT-AFABP most closely in sensing the negative charge, retaining virtually 100% sensitivity. K113I-AFABP (β-I strand) maintained 90% of the sensitivity to negative charge of the wild-type protein. Another nonportal mutant K10I-AFABP (β-A strand), however, showed a 40% decrease in the sensitivity to vesicle negative charge relative to wild-type AFABP ($p < 0.05$).

In general, the decreased sensitivity of the mutant proteins to the negatively charged membranes was parallel to their slower transfer rates relative to the wild-type proteins. In other words, the slower the absolute transfer rate in comparison with native AFABP, the less sensitive to membrane negative charge. In Figure 6, the relative transfer rate for each protein is shown as the ratio of the transfer rate to negatively charged vesicles to the transfer rate to zwitterionic vesicles. For native AFABP, which displays the most rapid 2AP transfer rates, the increase in rate to CL-incorporated membranes exceeded 50-fold. For the double mutant K22,59I, which has the slowest absolute fatty acid transfer rates of all proteins examined, the increase in rate to CL-containing membranes was less than 8-fold. An exception to this relationship was found for the K32I mutation. Mutant K32I-AFABP appeared to be relatively insensitive to negative charge, even though the absolute rates of 2AP transfer to PS vesicles were reduced only by 10−20% compared to those from wild-type AFABP. This was due to its more rapid AOFA transfer rates to neutral vesicles relative to the rates from the other proteins, including wild-type AFABP (Figure 2).

These studies suggest that lysines in the helical region of AFABP are important in sensing the negative charge of phospholipid membranes during the collisional process of FA transfer, showing generally more sensitivity than those out of the helical domain. In addition, lysine 32 on the αII-helix is, perhaps, involved in the FA transfer process in a unique way relative to other lysines: the K32I mutation resulted in a dramatic increase in AOFA transfer rate to zwitterionic vesicles (Figure 2), as well as a large decrease in AOFA transfer rate to anionic membranes (Figure 4), and almost no response was found to acceptor negative charge without the presence of positively charged K32 (Figure 5).

DISCUSSION

AFABP is thought to be important in the intracellular transport of unesterified FA. Previous studies have suggested that basic lysine residues on the surface of AFABP may

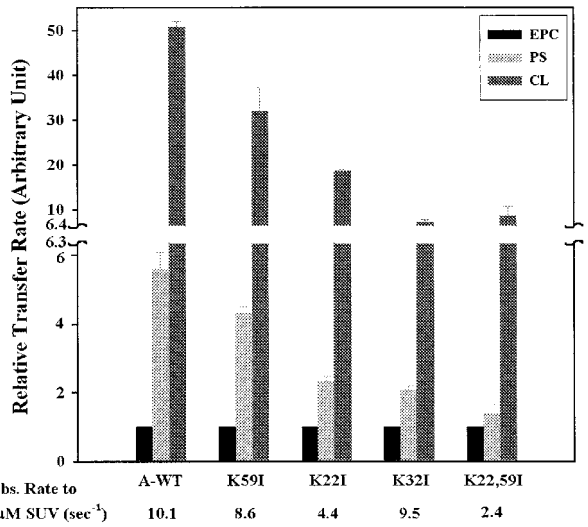

FIGURE 6: Effect of vesicle net charge on relative rate of AOFA transfer from AFABPs. Transfer of 1 μM 2AP from 10 μM native and mutant proteins to 100 μM vesicles with different phospholipid composition is shown. Key: EPC/NBDPC (black bar), EPC/NBDPC/PS (light gray bar), and EPC/NBDPC/CL (dark gray bar). Results are expressed relative to the average transfer rate of 2AP to neutral EPC/NBDPC membranes. The mean ± SEM is presented. The absolute rates of FA transfer from wild-type and mutant AFABPs to 100 μM PS vesicles are listed below the *x*-axis.

participate in electrostatic interactions between AFABP and phospholipid membranes that are proposed to occur during fatty acid transfer (*12*, *27*). On the basis of the well-known membrane-binding properties of amphipathic helices, we suggested that the helix−turn−helix domain of AFABP would be likely to be involved in potential AFABP−membrane interactions, since the αI-helix is amphipathic (*18*). The importance of the helical region of AFABP can also be inferred by comparison of the amino acid sequences for orthologous and paralogous FABP's (*41*). The first 39 residues of AFABP from the N-terminal end, which include the two α-helices that form the "lid" on the β-barrel as well as the β-A strand, are conserved in all species studied so far (*41*). This appears to place additional significance to this portion of the structure. The exact importance of the strict sequence identity at the N-terminus is not yet completely understood. Molecular dynamics simulation estimates have suggested that the α-helical domain is involved in maintaining the integrity of the internal binding site and enhancing ligand selectivity (*29*, *30*, *42*). In addition, these theoretical studies have suggested that the αII-helix functions in stabilizing the binding cavity of IFABP (*25*, *26*). In the present study, we focused on the role of the helix−turn−helix portal domain in FA transfer to membranes. We demonstrate that lysines in the first 39 residues, as well as K59, located in the β C-D turn of AFABP, are important determinants of the absolute rate of FA transfer to membranes. In addition, K22 and K32 in the αI- and αII-helices, respectively, are likely to be involved in electrostatic interactions with anionic phospholipids of acceptor membranes.

It was found that mutations of lysine to isoleucine did not significantly alter protein structural integrity. Since acetylation of all 14 lysine residues of AFABP was shown previously not to alter protein secondary structure and ligand-binding affinity when compared to native protein (*11*), we had expected that single site mutation would not introduce dramatic changes. This is also in agreement with another series of K → I point mutants of the homologous HFABP, examined in our laboratory, as well as those engineered by Veerkamp and colleagues (*27*, *43*). Indeed, the FABP β-barrel structure seems to be very stable, as a covalent modification did not influence folding (*44*) and since a variant of IFABP that lacks both of the α-helices still forms a stable structure and maintains the ligand-binding cavity (*25*, *45*, *46*).

Previously, changing lysine 22 of HFABP to a neutral or acidic residue yielded proteins that did not respond at all to the negative charge of membranes (*27*). For AFABP, in contrast, neutralization of no single lysine residue examined completely abolished the increase in FA transfer rate from protein to anionic compared with zwitterionic membranes. Nevertheless, we observed varying degrees in the loss of sensitivity to membrane charge, ranging from 30% to 85%, from point mutants with an isoleucine replacement in the portal region and the β-A strand. A number of recent observations are consistent with the hypothesis that the portal/helical domain of the FABP's is important in FA transport. Using protein structure calculations, Licata and Bernlohr examined the surface electrostatic potential of AFABP and showed that the protein has a strong ridge of positive potential across the helix−turn−helix region which extends to include the opening to the binding cavity (*47*). This is consistent with our transfer results, in that the positive electrostatic polarity in this domain may promote the binding of the protein to negatively charged membranes. Hence, these studies support the idea that a disruption in charge−charge interactions between positive lysines and the negative charges of membranes by the substitution of isoleucine for lysine contributes to the observed reductions in FA transfer rates.

Lysine 32 lies within the αII-helix, shown to be one of the most dynamic regions in backbone mobility by NMR spectroscopy and as predicted by computer simulations (*42*, *26*). Abolishment of the positive charge of K32 resulted in a unique pattern of FA transfer to membranes. Transfer was 2−3-fold faster to zwitterionic vesicles but up to 3-fold slower to PS and CL vesicles when compared to those from WT-AFABP. The large reduction in sensitivity to membrane charge suggests that lysine 32 is important in sensing the negative charge of the acceptor phospholipid membranes and that substitution of isoleucine for lysine at residue 32 disrupted electrostatic interaction of K32I-AFABP with membranes. The possible cause of the increase in rate to neutral vesicles was explored by an examination of side chain interactions. Previously, arginine 31 and aspartic acid 18 were speculated to form a salt bridge (*18*); however, their side chains do not extend toward each other, and no direct evidence to support this interaction has been reported. We propose, rather, that a local electrostatic interaction between lysine 32 and aspartic acid 18 on the αI-helix may help to hold the two helices together and therefore maintain the stability of the helical cap (Figure 7). Unlike the other 13 lysines of AFABP which have a stretched side chain facing the aqueous milieu, lysine 32 has a unique kinked positive side chain, oriented toward the carboxyl group of aspartic acid 18. The computer modeling program Insight II (Silicon Graphics, Inc.) was used to obtain the distance between the amino group of lysine 32 and the carboxylate group of

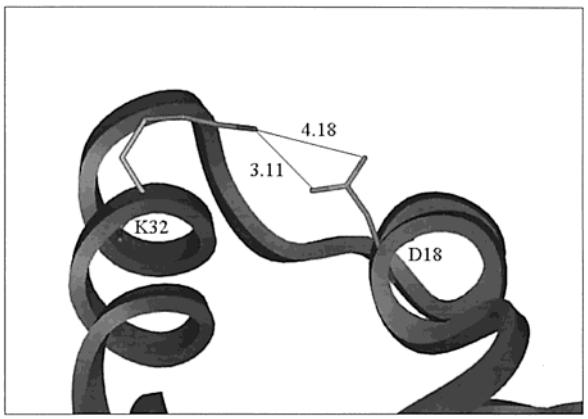

FIGURE 7: Atomic distances between K32 and D18. The distances between the nitrogen of lysine 32 and two individual oxygens of the aspartic acid 18 carboxylate group are shown as 3.11 and 4.18 Å, respectively. The one-letter abbreviations are shown on the backbone of amino acids, and the amino acids were numbered without the first methionine.

Table 5: Atomic Distance between the Amino Group of Lys 32 or Arg 31 and the Carboxylate Group of Asp 18[a]

AFABP amino acid	atom (N)	distance (Å) to atom (O) of Asp 18	
		OD1	OD2
Lys 32 (holo)	NZ	3.11	4.18
Arg 31 (holo)	NH1	5.53	5.39
	NH2	4.57	4.16
Lys 32 (apo)	NZ	2.95	4.23
Arg 31 (apo)	NH1	5.55	5.30
	NH2	4.61	4.03

[a] Distances were determined using the computer program Insight II (Silicon Graphics, Inc.) (*18*). The protein code of AFABP is "1lid" with oleate bound inside the binding pocket. NZ represents the nitrogen atom in the amino group of the lysine residue. NH1 and NH2 represent nitrogen atoms from each amino group of arginine. OD1 and OD2 represent oxygen atoms from the carboxylate group of aspartic acid 18.

aspartic acid 18, and these were found to be generally smaller than distances between arginine 31 and aspartic acid 18 (Table 5 and Figure 7). Therefore, it is possible that a salt bridge forms between K32 and D18, contributing to the stability of the two helices. The role of surface salt bridges to local and overall protein stability has been described in other proteins (*48*, *49*). A helical cap which lacks this salt bridge, e.g., caused by a K32 → I32 mutation, resulted in a faster FA transfer rate to neutral acceptor vesicles. In the case of FA transfer to acidic phospholipid-containing vesicles, however, the overall electrostatic interaction between the protein and membranes appears to be a more dominant factor than the local K32−D18 interaction. This charge−charge interaction, then, overrides the local interaction in determining the absolute rate of fatty acid transfer; therefore, a decrease in transfer rates to negatively charged vesicles was observed due to the abolishment of positive charge in the protein.

These suggestions are consistent with our previous hypothesis that the FA collisional transfer mechanism is likely to be a multistep process (*50*), as follows: The first step may be governed by electrostatic interactions involving the entire helical lid of the protein with the acceptor phospholipid membranes. This interaction is proposed, in turn, to induce a conformational change in the putative cap, from an ordered closed state to a disordered open state. The protein then releases the LCFA from its internal ligand binding cavity, and finally, the FA associates with the acceptor membrane. Thus, an isoleucine replacement for lysine at residue 32 could cause a decrease in electrostatic interactions of the helical lid and may also alter the conformational state of the putative cap. At present, the rate-limiting step in this putative FA transfer sequence is not known. Estimates of FA on-rates to membranes suggest that this step occurs very rapidly, and thus is not likely to be rate determining (*51*). Dissociation of FA from the FABP-binding site may not be equivalent for the protein in solution compared to a protein−membrane "collisional complex"; nevertheless, since the point mutations did not substantially alter the FA-binding affinities, the dissociation of the ligand is also not likely to be rate limiting. Thus, it is possible that binding of AFABP to the membrane and/or conformational changes in AFABP induced by membrane interaction may determine the overall rate of ligand transfer.

Amphipathic helices are known to be involved in protein−lipid interactions, and the significance of amphipathic helices in protein targeting to membranes has been studied extensively (*52*). A major determinant of binding to lipid surfaces is the ability of the amphipathic peptide to attain the correct orientation of hydrophobic and hydrophilic groups (*53*, *54*). The αI-helix of AFABP is amphipathic. Thus, the K22I mutation could slightly alter the helical content of the region and/or alter its relative hydrophilicity, resulting in a decrease in the rate of FA transfer. On the basis of the transfer results obtained with the K22I-AFABP mutant, it appears that K22 of AFABP is necessary for the formation of effective electrostatic interactions between AFABP and membrane acidic phospholipids. These results are consistent with our previous series of isoleucine substitution mutagenesis in HFABP, where the K22I mutation also resulted in a dramatic decrease in absolute AOFA transfer rate and a decrease in sensitivity to membrane negative charge (*27*). Thus, by disrupting AFABP−membrane electrostatic interactions, mutation of this lysine may interrupt the targeting of the helical lid to membranes, which then decreases the rate of FA transfer.

The β-turn between strands C and D (residues 57−60) is another region considered to be part of the portal domain. In the present study, mutation K59I led to an approximately 50% decrease in the rate of FA transfer relative to wild-type AFABP. Along with the αII-helix, residues 56−59 also exhibit a high degree of conformational freedom, as determined by *B* factors in X-ray crystallographic studies, backbone and side chain dynamics obtained by NMR, and molecular dynamics simulations (*18*, *29*, *30*, *41*, *55*). The β C-D turn is suggested to interact with the αII-helix to cap the ligand-binding cavity (*30*) and was also proposed to be involved in ligand binding, since the side chain of K59 is found within 4 Å proximity to the bound ligand (*41*). Moreover, lysine 59 was also shown to form a hydrogen bond with a water molecule in the binding cavity, and this was proposed to play a role in the stability of protein folding. Interaction with the bound water may also play a role in buffering ligand binding and release without causing major changes in the binding cavity (*41*). Mutation of this lysine could therefore result in disrupted ligand binding and/or a disordered environment in the ligand-binding cavity, which

could decrease the binding affinity of FA to AFABP. However, we did not observe this phenomenon, and if anything, the binding affinity was actually slightly increased (Table 2). Thus, the decreased rate of 2AP transfer from K59I-AFABP is likely primarily explained by the disruption of charge−charge interactions between the AFABP surface and the acceptor membranes, brought about by changes in the surface electrostatic properties of the protein.

To elucidate whether additional domains are involved in the collisional transfer process, we constructed three K → I mutants in regions outside the portal region, specifically on β-A, -G, and -I strands. These mutations also altered the 2AP transfer rate; however, the reduction in rates was generally small compared with that in the portal mutants. The mutations in strands G and I (K97I and K113I) resulted in 5−35% slower transfer but did not affect the sensitivity of the transfer rate to anionic membrane phospholipids. For the mutation in strand A (K10I), however, absolute AOFA transfer rates were 20−45% lower than from native AFABP, and sensitivity to anionic phospholipid was reduced by approximately one-third. Unlike HFABP, the nonportal mutants of AFABP cannot be considered purely as negative controls, and the results imply that the surface of the β-barrel structure of AFABP may also contribute to the regulation of FA transport, albeit to a lesser extent in comparison with the portal region of the protein.

The helical domain may also, in part, underlie functional differences between AFABP and HFABP, for example, the faster AOFA transfer from AFABP. HFABP contains no lysine in the αII-helix, whereas AFABP contains K32. Introduction of a lysine residue into the αII-helix of HFABP (T28K-HFABP) resulted in a faster FA transfer rate relative to native HFABP and a more sensitive response to membrane charge, both properties more similar to AFABP.

No single mutation generated altered the ligand transfer mechanism of the proteins from collision-based to diffusional. Thus, the collisional interaction between AFABP and membrane is not likely to be dependent on only one residue or domain of the protein. Overall, it appears that the helix−turn−helix element had a greater impact on FA transfer than the other regions. Lysine 22 (and/or helix I) is important in establishing the rate of FA transfer and sensing the membrane negative charge. Lysine 32 (and/or helix II) may be particularly important in sensing the negative charge of acceptor membranes as well as in stabilizing the helix−turn−helix conformation. Lysines 10 and 59 also play a role in the FA transfer process. In conclusion, the helical domain and the β C-D turn, all components of the putative ligand portal region, along with the β-A strand, appear to be the likely structural elements responsible for the physical interactions between AFABP and membranes which occur during the process of FA transfer.

ACKNOWLEDGMENT

We thank Dr. Peter C. Kahn and Mr. John K. Everett (Department of Biochemistry and Microbiology, Rutgers University) for their invaluable assistance with the protein energy minimization studies.

REFERENCES

1. Spiegelman, B. M., and Green, H. (1980) *J. Biol. Chem. 255*, 8811−8818.
2. Gregoire, F. M., Smas, C. M., and Sul, H. S. (1998) *Physiol. Rev. 78*, 783−809.
3. Sha, R. S., Kane, C. D., Xu, Z., Banaszak, L. J., and Bernlohr, D. A. (1993) *J. Biol. Chem. 268*, 7886−7892.
4. Waggoner, D. W., and Bernlohr, D. A. (1990) *J. Biol. Chem. 265*, 11417−11420.
5. Trigatti, B. L., Mangroo, D., and Gerber, G. E. (1991) *J. Biol. Chem. 266*, 22621−22625.
6. Shen, W.-J., Sridhar, K., Bernlohr, D. A., and Kraemer, F. B. (1999) *Proc. Natl. Acad. Sci. U.S.A. 96*, 5528−5532.
7. Kim, H. K., and Storch, J. (1992) *J. Biol. Chem. 267*, 20051−20056.
8. Hsu, K.-T., and Storch, J. (1996) *J. Biol. Chem. 271*, 13317−13323.
9. Kim, H. K., and Storch, J. (1992) *J. Biol. Chem. 267*, 77−82.
10. Herr, F. M., Li, E., Weinberg, R. B., Cook, V. R., and Storch, J. (1999) *J. Biol. Chem. 274*, 9556−9563.
11. Wootan, M. G., and Storch, J. (1994) *J. Biol. Chem. 269*, 10517−10523.
12. Herr, F. M., Matarese, V., Bernlohr, D. A., and Storch, J. (1995) *Biochemistry 34*, 11840−11845.
13. Gericke, A., Smith, E. R., Moore, D. J., Mendelsohn, R., and Storch, J. (1997) *Biochemistry 36*, 8311−8317.
14. Smith, E. R., and Storch, J. (1999) *J. Biol. Chem. 274*, 35325−35330.
15. Banaszak, L., Winter, N., Xu, Z., Bernlohr, D. A., Cowan, S., and Jones, T. A. (1994) *Adv. Protein Chem. 45*, 89−151.
16. Glatz, J. F. C., and van der Vusse, G. J. (1996) *Prog. Lipid Res. 35*(3), 243−282.
17. Xu, Z., Bernlohr, D. A., and Banaszak, L. J. (1992) *Biochemistry 31*, 3484−3492.
18. Xu, Z., Bernlohr, D. A., and Banaszak, L. J. (1993) *J. Biol. Chem. 268*, 7874−7884.
19. Hunt, C. R., Ro, J. H., Dobson, D. E., Min, H. Y., and Spiegelman, B. M. (1986) *Proc. Natl. Acad. Sci. U.S.A. 83*, 3786−3790.
20. Bernlohr, D. A., Angus, C. W., Lane, M. D., Bolanowski, M. A., and Kelley, T., Jr. (1984) *Proc. Natl. Acad. Sci. U.S.A. 81*, 5468−5472.
21. Storch, J., and Thumser, A. E. (2000) *Biochim. Biophys. Acta 1486*, 28−44.
22. Zanotti, G., Scapin, G., Spadon, P., Veerkamp, J. H., and Sacchettini, J. C. (1992) *J. Biol. Chem. 267*, 18541−18550.
23. Sacchettini, J. C., Gordon, J. I., and Banaszak, L. J. (1988) *J. Biol. Chem. 263*, 5815−5819.
24. Thompson, J., Winter, N., Terwey, D., Bratt, J., and Banaszak, L. (1997) *J. Biol. Chem. 272*, 7140−7150.
25. Hodsdon, M. E., and Cistola, D. P. (1997) *Biochemistry 36*, 1450−1460.
26. Hodsdon, M. E., and Cistola, D. P. (1997) *Biochemistry 36*, 2278−2290.
27. Herr, F. M., Aronson, J., and Storch, J. (1996) *Biochemistry 35*, 1296−1303.
28. Wootan, M. G., Bernlohr, D. A., and Storch, J. (1993) *Biochemistry 32*, 8622−8627.
29. Woolf, T. B. (1998) *Biophys. J. 74*, 681−693.
30. Woolf, T. B., and Tychko, M. (1998) *Biophys. J. 74*, 694−707.
31. Higuchi, R., Krummel, B., and Saiki, R. K. (1986) *Nucleic Acids Res. 16*, 7351−7367.
32. Sanger, F., Coulson, A. R., Barrell, B. G., Smith, A. J. H., and Roe, B. A. (1980) *Mol. Biol. 143*, 161−178.
33. Richeri, G. V., Ogata, R. T., and Kleinfeld, A. M. (1994) *J. Biol. Chem. 269*, 23918−23930.
34. Yang, J. T., Wu, C. S., and Martinez, H. M. (1986) *Methods Enzymol. 130*, 208−269.
35. Chang, C. T., Wu, C.-S. C., and Yang, J. T. (1978) *Anal. Biochem. 91*, 13−31.
36. Wootan, M. G., Bass, N. M., Bernlohr, D. A., and Storch, J. (1990) *Biochemistry 29*, 9305−9311.
37. Richeri, G. V., Anel, A., and Kleinfeld, A. M. (1993) *Biochemistry 32*, 7574−7580.
38. Huang, C., and Thompson, T. E. (1974) *Methods Enzymol. 32*, 485−489.

39. Gomori, G. (1942) *J. Lab. Clin. Med. 27*, 955−960.
40. Richieri, G., Low, P. J., Ogata, R. T., and Kleinfeld, A. M. (1998) *J. Biol. Chem. 273*, 7397−7408.
41. Reese-Wagoner, A., Thompson, J., and Banaszak, L. (1999) *Biochim. Biophys. Acta 1441*, 106−116.
42. Constantine, K. L., Friedrichs, M. S., Wittekin, M., Jamil, H., Chu, C.-H., Parker, R. A., Goldfarb, V., Mueller, L., and Farmer, B. T., II (1998) *Biochemistry 37*, 7965−7980.
43. Zimmerman, A. W., Rademacher, M., Rüterjans, H., Lücke, C., and Veerkamp, J. H. (1999) *Biochem. J. 344*, 495−501.
44. Frieden, C., Jiang, N., and Cistola, D. P. (1995) *Biochemistry 34*, 2724−2730.
45. Cistola, D. P., Kim, K., Rogl, H., and Frieden, C. (1996) *Biochemistry 35*, 7559−7565.
46. Kim, K., Cistola, D. P., and Frieden, C. (1996) *Biochemistry 35*, 7553−7558.
47. LiCata, V. J., and Bernlohr, D. A. (1998) *Proteins 33*, 577−589.
48. Hennig, M., Darimont, B., Kirschner, K., and Jansonius, J. N. (1995) *Structure 3*, 1295−1306.
49. Yip, K. S., Stillman, T. J., Britton, K. L., Artymiuk, P. J., Baker, P. J., Sedelnikova, S. E., Engel, P. C., Pasquo, A., Chiaraluce, R., and Consalvi, V. (1995) *Structure 3*, 1147−1158.
50. Corsico, B., Cistola, D. P., Frieden, C., and Storch, J. (1998) *Proc. Natl. Acad. Sci. U.S.A. 95*, 12174−12178.
51. Storch, J., and Kleinfeld, A. M. (1986) *Biochemistry 25*, 1717−1726.
52. Anantharamaiah, G. M., Jones, M. K., and Segrest, J. P. (1993) in *The Amphipathic Helix* (Epand, R. M., Ed.) pp 110−143, CRC Press, Boca Raton, FL.
53. Hammen, P. K., Gorenstein, D. G., and Weiner, H. (1996) *Biochemistry 35*, 3772−3781.
54. Roise, D. (1993) in *Thermodynamics of Membrane Receptors and Channels* (Jackson, M. B., Ed.) pp 81−125, CRC Press, Boca Raton, FL.
55. Rich, M. R., and Evans, J. S. (1996) *Biochemistry 35*, 1506−1515.

BI0101042